Full-Scale Testing of Allan Edwards Compression Sleeve

Final Report

Prepared for Allan Edwards, Inc.

Report No. 100301-RP01-Rev2-040622

April 2022

Testing performed by ADV Integrity, Inc.

Full-Scale Testing of Allan Edwards Compression Sleeve

Final Report

Prepared for

Allan Edwards, Inc.

Tulsa, OK

April 2022

Prepared by:



David Futch, PE
david.futch@advintegrity.com

Prepared by:



Atul Ganpatye, PE
atul.ganpatye@advintegrity.com

Reviewed by:



Dr. Chris Alexander, PE
chris.alexander@advintegrity.com

100301-RP01-Rev2-040622

Rev	Date	Description	Prepared	Checked	Reviewed
B	01.13.2022	Issued for Client Review	DBF	AG	CRA
0	01.21.2022	Issued as Final	DBF	AG	CRA
1	04.04.2022	Updated with Additional Testing	DBF	AG	CRA
2	04.06.2022	Issued as Final	DBF	AG	CRA

Texas Registered Engineering Firm F-19081
www.advintegrity.com

Monday, April 6, 2022 100301-RP01-Rev2-040622

Josh Wilson
Allan Edwards, Inc.
6468 N. Yale Ave.
Tulsa, OK 74117

Josh,

Enclosed is our report documenting the recent full-scale testing program of the Allan Edwards Compression Sleeve system utilizing induction heating. This program included full-scale fatigue testing of repaired samples and additional numerical modeling to better understand the complexities of a repair using the Compression Sleeve. These results are

summarized in the following report.

Thank you for the opportunity to complete this work. Please do not hesitate to contact us with any questions.

Regards,



David Futch, PE | Senior Associate

ADV Integrity, Inc.
28246 FM 2920 | Waller, TX 77484
Office: (832) 409-4529 **|** E-mail: david.futch@advintegrity.com
Texas Registered Engineering Firm F-190

Reviewed by: Dr. Chris Alexander, PE | President

CONTENTS

1.0 Introduction and Background 4
2.0 Mock-Up Tests 6
3.0 Full-Scale Testing 12
3.1 Sample Geometry 12
3.2 Test Plan 12
3.3 Test Results 16
3.4 Metallurgical Examination 19
4.0 Numerical Modeling 21
4.1.1 Pipe and Sleeve Stress Analysis - Concept 21
4.2 Finite Element Modeling and Analysis 22
4.3 Results and Discussion 23
4.4 Interpretation of Measured Gap Data for Estimating Sleeve Performance 29
5.0 Discussion and Summary 30

LIST OF FIGURES

Figure 2-1: Example photograph of tapered gap gage. 9
Figure 2-2: Strain gage and thermocouple configuration during mock-up tests. 9
Figure 2-3: Plot of strain vs time during clamp actuation. 10
Figure 2-4: Plot of temperature vs time with an induction heater output of 35 kW. 10
Figure 2-5: Plot of temperature vs time with an induction heater output of 28 kW. 11
Figure 2-6: Plot of temperature vs time with an induction heater output of 20 kW. 11
Figure 3-1: Photograph during heat tinting of EDM notch after completing pre-cycling. 13
Figure 3-2: Photograph of hardenable fill install at notch location. 14
Figure 3-3: Photograph of induction heater set-up. 14
Figure 3-4: Photograph of long seam welding. 15
Figure 3-5: Schmatic showing location of strain gages, thermocoupoes, and EDM notch. 15
Figure 3-6: Strain and temperature vs time measured during the install of Sleeve 1. 17
Figure 3-7: Strain and temperature vs time measured during the install of Sleeve 2. 17
Figure 3-8: Strain and temperature vs time measured during the install of Sleeve 3. 18
Figure 3-9: Strain and temperature vs time measured during the install of Sleeve 4. 18
Figure 3-10: Pressure vs time measured during burst testing of surviving samples. 19
Figure 3-11: Notch from Sample 1. Major numbered scale divisions are inches. 20
Figure 3-12: Notch from Sample 2. Major numbered scale divisions are inches. 20
Figure 3-13: Notch from Sample 3. Major numbered scale divisions are inches. 20
Figure 3-14: Notch from Sample 4. Major numbered scale divisions are inches. 20
Figure 4-1: Concept of interface pressure between the pipe and the sleeve 21
Figure 4-2: Schematic of the FEA model 23
Figure 4-3: Stress profiles due to temperature differentials, $\Delta T = 166\ ^{o}F$ 24
Figure 4-4: Stress profiles due to temperature differentials + pressure, $\Delta T = 166\ ^{o}F$, P = 1104 psig 25
Figure 4-5: Comparison of stress profiles – temperature + pressure vs only temperature, $\Delta T = 166\ ^{o}F$ 26
Figure 4-6: Stress profiles due to temperature differentials, $\Delta T = 316\ ^{o}F$ 26
Figure 4-7: Stress profiles due to temperature differentials + pressure, $\Delta T = 316\ ^{o}F$, P = 1104 psig 27
Figure 4-8: Comparison of stress profiles – temperature + pressure vs only temperature, $\Delta T = 316\ ^{o}F$ 27
Figure 4-9: Summary of FEA results for pipe and sleeve stresses at various temperature differentials 28
Figure 4-10: Summary of FEA results for pipe and sleeve stresses – verification 28
Figure 5-1: Possibility of base pipe ovalization during clamping of the sleeve on the base pipe 31

LIST OF TABLES

Table 2-1: Time and Temperature Differential 8
Table 2-2: Summary of Gaps Measured 8
Table 3-1: Sample Configuration 12
Table 3-2: Summary of Test Results 16
Table 3-3: Summary of Crack Depths 19
Table 4-4: Summary of Calculated Stresses in the Pipe and the Sleeve Using Measured Gap Data 29
Table 5-1: Annual Cyclic Pressure Conditions Based on Kiefner Study Industry Survey 30

1.0 INTRODUCTION AND BACKGROUND

Allan Edwards contracted ADV Integrity, Inc. (ADV) to provide engineering and full-scale testing for developing a Type A compression sleeve starting in 2019, identified as the "Compression Sleeve". While there has been significant work developing and testing the compression sleeve, based on feedback from several pipeline companies there are several outstanding technical elements associated with the Compression Sleeve prior to Allan Edwards marketing this technology to pipeline operators to ensure its successful deployment.

ADV provided full-scale testing, numerical modeling, and engineering oversight during the assessment program. Allan Edwards provided the steel sleeves, equipment needed to install the sleeves, and oversight during the installation. ADV understands that Allan Edwards will use the test results detailed in the this report to update their internal application procedures.

Upon completion of this test scope, ADV's goal is to:

- Document that the reinforced carrier pipe is fully in compression at the maximum operating pressure, as this condition provides a simplified approach to eliminate fatigue crack growth.
- Develop the framework to facilitate reliable installs occur in the field and detailed quality control procedure steps to ensure repeatable results are achieved from one install to another.
- Provide sufficient confidence from field measurements and quality control procedures that the carrier pipe achieves compression.

The goal of any Type A compression sleeve should be to meet the requirements of CSA Z662, Section 10.11.4.4. CSA Z662 is unique as it explicitly calls out a Type A compression sleeve as a repair option. Therefore, it provides the most comprehensive set of requirements accepted by a regulator of all pipeline codes (i.e., ASME B31.4, ASME B31.8, ASME PCC-2, etc.).

In addition to the requirements of Clause 10.11.4.1, steel compression reinforcement repair sleeves shall be subject to the following requirements:

a) The sleeve system shall be designed and tested to satisfy the following over the expected range of operating conditions:
   i. A compressive hoop stress shall be maintained in the carrier pipe at the location of the defect.
   ii. The hoop stress in the sleeve shall not exceed its maximum design stress.
   iii. Any filler used between the carrier pipe and the sleeve shall transfer the force from the sleeve to the carrier pipe, cure at the temperature existing following the sleeve installation prior to normal operation, and not be subject to deterioration under pipeline design operating conditions.

b) The sleeve system installation method shall satisfy the following:
   i. The method shall ensure that the steel in the vicinity of the defect remains in compression over the full pressure and temperature range expected during operation of the pipeline and that the stress level in the defect region is reduced to arrest defect growth and deterioration.
   ii. The sleeve system shall be used only where its installation prevents further growth or deterioration of the defects under the sleeve.
   iii. Where a sleeve is to be installed over a circumferential or mill seam weld with a protruding weld cap, excessive weld cap material shall be removed, or the sleeves shall be grooved, to

prevent stress concentrations at the weld locations. Any resultant reduction in wall thickness of the sleeve shall be considered in determining the maximum stress in the sleeve.

iv. Personnel installing sleeves shall be competent in the installation procedures by the sleeve manufacturer or supplier, or by personnel who have been so trained and qualified.

v. Welds used to join the two halves of the sleeve together shall be as specified in Clause 7.

c) An engineering assessment shall be undertaken to verify the installation parameters and inspection method used. The following factors shall be considered:

i. pipe and sleeve design;
ii. pipe and sleeve material properties;
iii. pipe and sleeve cleanliness;
iv. expected service conditions;
v. residual or external stresses;
vi. internal pipe pressure during installation;
vii. cleaning of the pipe;
viii. heating of the sleeve prior to welding;
ix. flow rate and heat transfer coefficient of the service fluid in the pipeline;
x. sleeve clamping methodology;
xi. welding procedures and welding qualifications; and
xii. testing the factors in Items i. to xi.

To accomplish the above goals, ADV structured a test scope in four (4) phases as described below and in the following report:

(1) Mock-up Tests to verify the ability of the Compression Sleeve configuration to achieve compression
(2) Limited Full-Scale Testing
(3) Limited Numerical Modeling and/or Calculations
(4) Reporting and Updating Excel-based Calculator.

2.0 MOCK-UP TESTS

Prior to completing the full-scale tests, ADV designed a series of mock-up tests to replicate a compression sleeve installation. The goal of this mock-up test was to better characterize the ability of the sleeve configuration to achieve a temperature differential between the sleeve/pipe and monitor strain on the inside pipe surface during installation. Initially these mock-ups were completed using a nominal 12.75-inch OD x 0.188-inch WT pipe and a 0.375-inch WT tight fitting sleeve. Later, additional mock-up tests were performed on nominal 24-inch OD x 0.312-inch WT pipe and a 0.375-inch WT tight fitting sleeve to better understand and correlate the heating temperature to the experienced sleeve gap before and after heating. The installation occurred using an open-ended pipe allowing access to the internal pipe surface during the installation process.

Initially, four total trials were performed, described below:

(1) Monitoring strain developed when actuating the clamps up to 4,000 psi.

(2) Monitoring the temperature differential between the pipe's internal surface and the sleeve's external surface when the induction heating unit has an output of 35 kW.

(3) Repeat (2), however, change induction heating unit output to 28 kW.

(4) Repeat (2), however, change induction heating unit output to 20 kW.

Later, six additional trials were performed to measure the evolution in the sleeve gap using a tapered gap gage, shown in Figure 2-1, described below:

(1) Install on a nominal 12.75-inch OD x 0.188-inch WT pipe

(2) Install on second nominal 12.75-inch OD x 0.188-inch WT pipe

(3) Install on nominal 24-inch OD x 0.312-inch WT pipe

(4) Repeat (1) through (3) by rotating sleeve approximately 45° and repeating installation

Strain gage and thermocouple locations are shown in Figure 2-2 and results from the clamp trail are presented in Figure 2-3. It's important to note that the strain measured here is only from actuating the clamps. Additional strain would be imparted from the heating and cooling of the sleeve; however, the main intent of this mock-up test is to quantify where and how strain develops while actuating the clamps. Clamps were installed to the outside surface of the sleeve three inches from either sleeve end and actuated to 4,000 psi (load specified in Allan Edwards Compression Sleeve application procedure) and then released. This process was repeated three (3) times. These results show that only actuating the clamp results in a compressive strain at the 45° gage location, whereas a tensile strain was measured at the 0° and 90° gage location. Gages directly below the clamp appear to result in larger magnitude strains (either

compressive or tensile). These results may change as a result of differences in pipe ovality and/or sleeve/pipe fit-up.

Results from the three temperature differential trails are presented in Figure 2-4 through Figure 2-6 for induction heater outputs of 35 kW, 28 kW, and 20 kW, respectively. These results show several key pieces of data:

(1) Time required to achieve approximately 400 °F on the outside surface of the pipe, a temperature required by the Allan Edwards installation procedure. Presumably, shorter time periods are advantageous as this allows for a shorter temperature soak time – resulting in a larger temperature differential.

(2) Temperature differential achieved between the outside surface of the sleeve and inside surface of the pipe when the outside surface of the sleeve reaches approximately 400 °F.

It should be noted that the induction heating unit was set at 400 °F and four spring loaded thermocouples were wired to the induction heating unit. Although the induction heater thermocouples may read 400 °F, the sleeve may achieve a greater temperature due to the induction fields and how those interact with the sleeve/pipe. Therefore, the thermocouple placed along the middle of the sleeve length at the top of the pipe (0°) resulted in a temperature greater than 400 °F. Also noteworthy, thermocouples installed on the top of the sleeve (0°) recorded temperatures approximately 100 °F hotter than the thermocouple on the bottom of the sleeve (180°) and approximately 150 °F hotter than the thermocouple on the side of the sleeve (90°). This temperature variation is likely due to the geometry of the induction blanket where the top rests snug against the sleeve surface, the bottom is dependent on the ability of the straps to hold the blanket against the sleeve, and the sides were not covered by the blanket.

Time to reach 400 °F and the temperature differential for the three induction heater outputs are shown in Table 2-1. The higher induction heater output resulted in a faster time to reach 400 °F, which consequently resulted in a larger temperature differential. A larger temperature differential is advantageous as it can result in increased compressive strain in the carrier pipe from thermal contraction. Therefore, the optimal induction heater output appears to be 35 kW.

Sleeve gaps were measured using a tapered gap gage during the second set of mock-ups. Sleeves were installed, clamps were tightened to 4,000 psi, and the first set of measurements were taken. Clamps were released to 1,000 psi and a second set of measurements were taken. At that time, the induction heating unit was turned on. The clamps were tightened to 4,000 psi once the temperature reached 400 °F, then a final set of measurements were conducted. These measurements are summarized in Table 2-2. The collected strain gage data was largely inconclusive, therefore, the performance of the sleeve was based upon the measured sleeve gaps, pre- and post-heat.

Table 2-1: Time and Temperature Differential

Induction Heater Output (kW)	Time to 400 °F (min:sec)[1]	Max Temperature Differential (°F)[2]
35	6:30	230
28	7:00	150
20	7:45	175

[1] 400 °F as measured by induction heater thermocouples, induction heater was shut off once 400 °F was achieved.
[2] Temperature differential for thermocouples installed at the top of the test specimen (0°) determined at the time the induction heater was shut off which would correlate to tacking the sleeve, locking in potential thermal expansion/contraction.

Table 2-2: Summary of Gaps Measured

Sample			Sleeve Gap (in) Measured at Clamp Pressure (psi)			Gap Δ, each side (in)	Total Average Gap Δ (in)
OD	#	Side	4,000 Cold Reading	1,000 Cold Reading	4,000 Hot Reading		
24 inch	1	Side A	0.041, 0.090,	0.041, 0.090,	0.024, 0.048,	0.017, 0.042,	0.050
		Side B	0.070, 0.054	0.071, 0.064	0.046, 0.036	0.025, 0.028	
	2	Side A	0.108, 0.140,	0.108, 0.141,	0.075, 0.115,	0.033, 0.026,	0.050
		Side B	0.140, 0.153	0.141, 0.153	0.112, 0.140	0.029, 0.013	
12 inch	1	Side A	0.085, 0.097,	0.089, 0.097,	0.058, 0.055,	0.031, 0.042,	0.063
		Side B	0.041, 0.036	0.043, 0.037	0.010, 0.010	0.033, 0.027	
	2	Side A	0.088, 0.040,	0.088, 0.040,	0.045, 0.015,	0.043, 0.025,	0.048
		Side B	0.030, 0.060	0.030, 0.064	0.027, 0.036	0.003, 0.028	
	3	Side A	0.113, 0.105,	0.111, 0.105,	0.074, 0.039,	0.037, 0.066,	0.084
		Side B	0.043, 0.045	0.043, 0.046	0.015, 0.010	0.028, 0.036	
	4	Side A	0.055, 0.095,	0.055, 0.095,	0.022, 0.049,	0.033, 0.046,	0.066
		Side B	0.033, 0.034	0.033, 0.036	0.009, 0.005	0.024, 0.031	

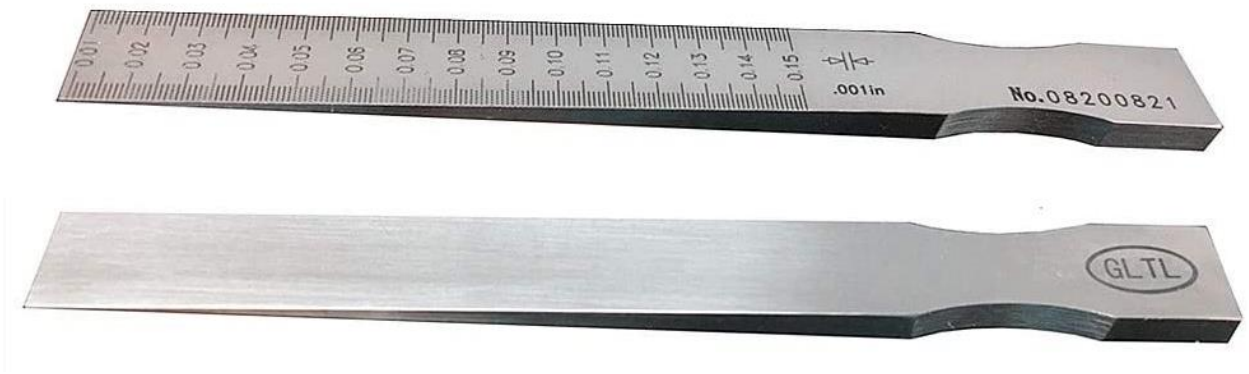
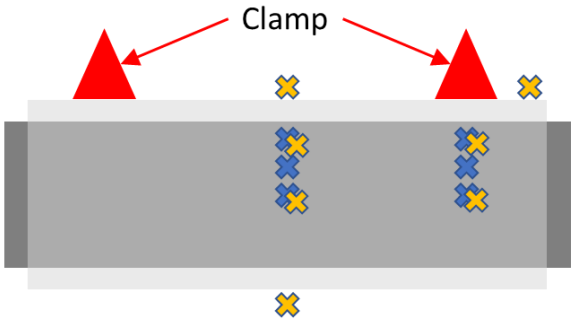
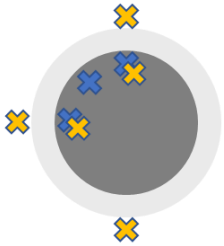


Figure 2-1: Example photograph of tapered gap gage.





Internal Surface Biaxial Strain Gages:

- Middle of sleeve and middle of clamp
- Positioned at 0° (top), 45°, and 90° (side)

Thermocouples:

- External: Middle of sleeve positioned at 0° (top), 90° (side), and 180° (bottom)
- External: Edge of sleeve positioned at 0° (top)
- Internal: Middle of sleeve and under clamp 0° (top) and 90° (side)

Figure 2-2: Strain gage and thermocouple configuration during mock-up tests.

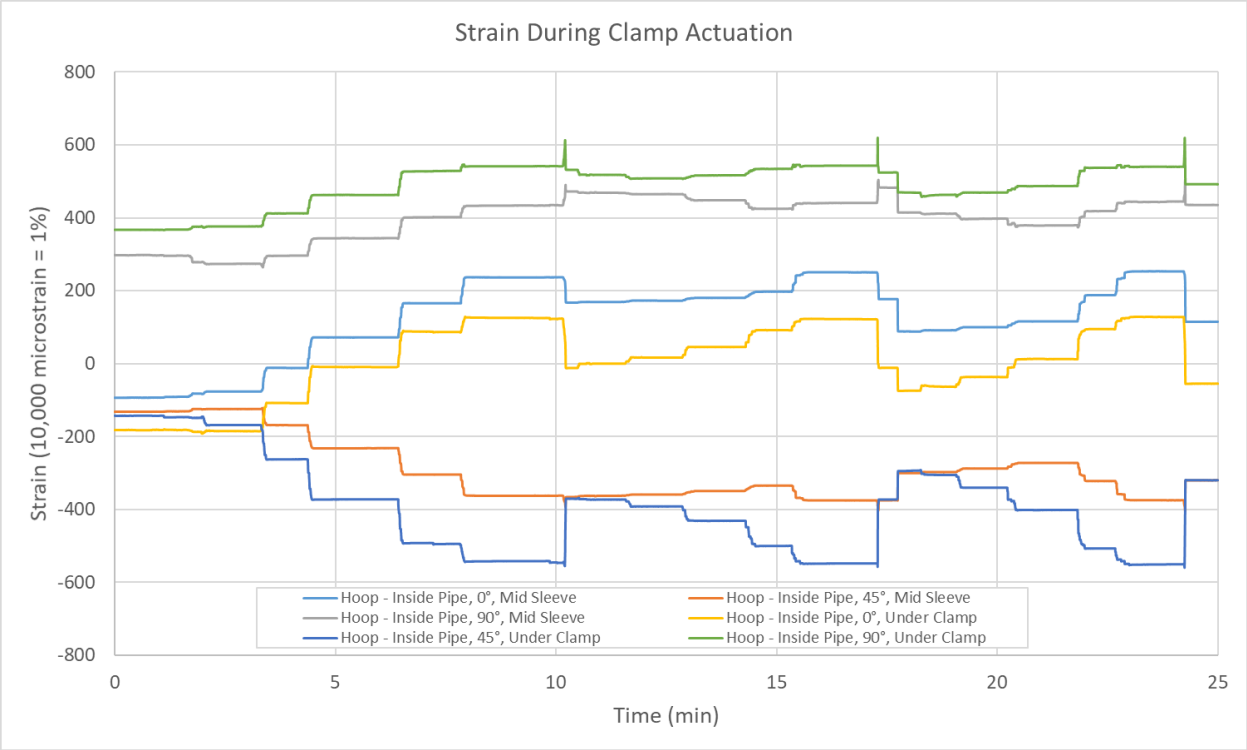


Figure 2-3: Plot of strain vs time during clamp actuation.

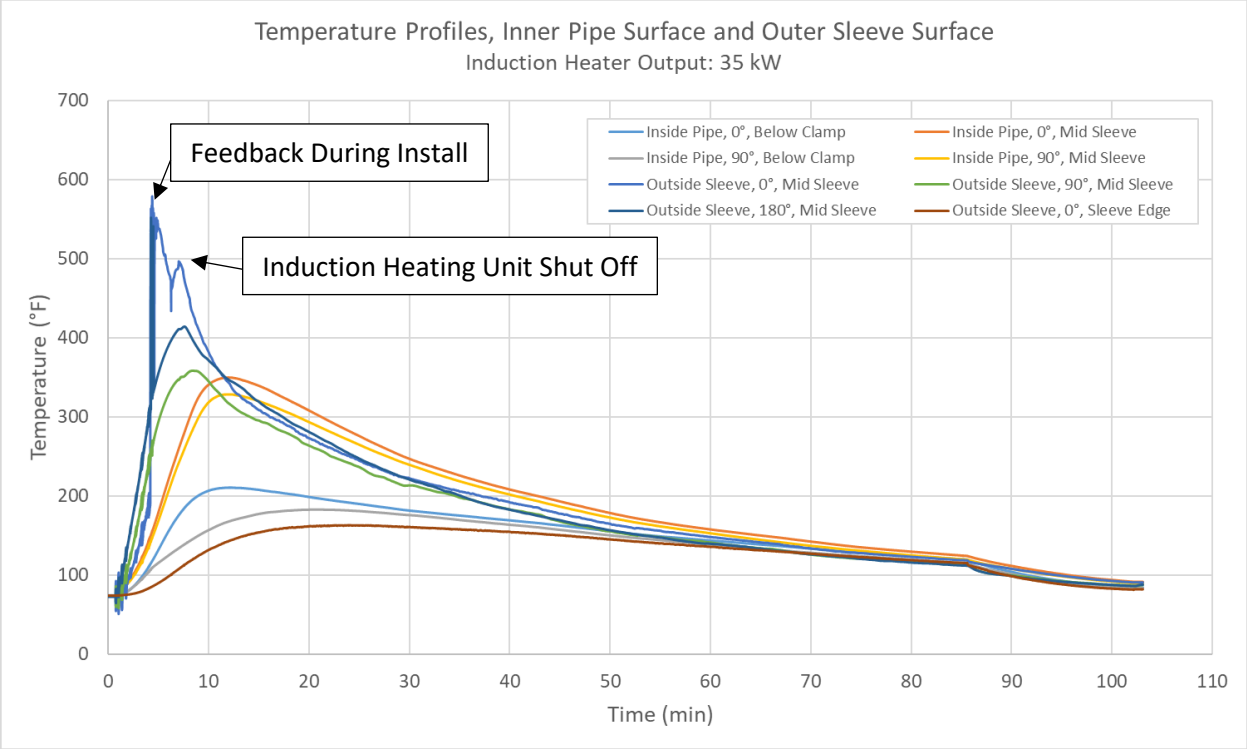


Figure 2-4: Plot of temperature vs time with an induction heater output of 35 kW.

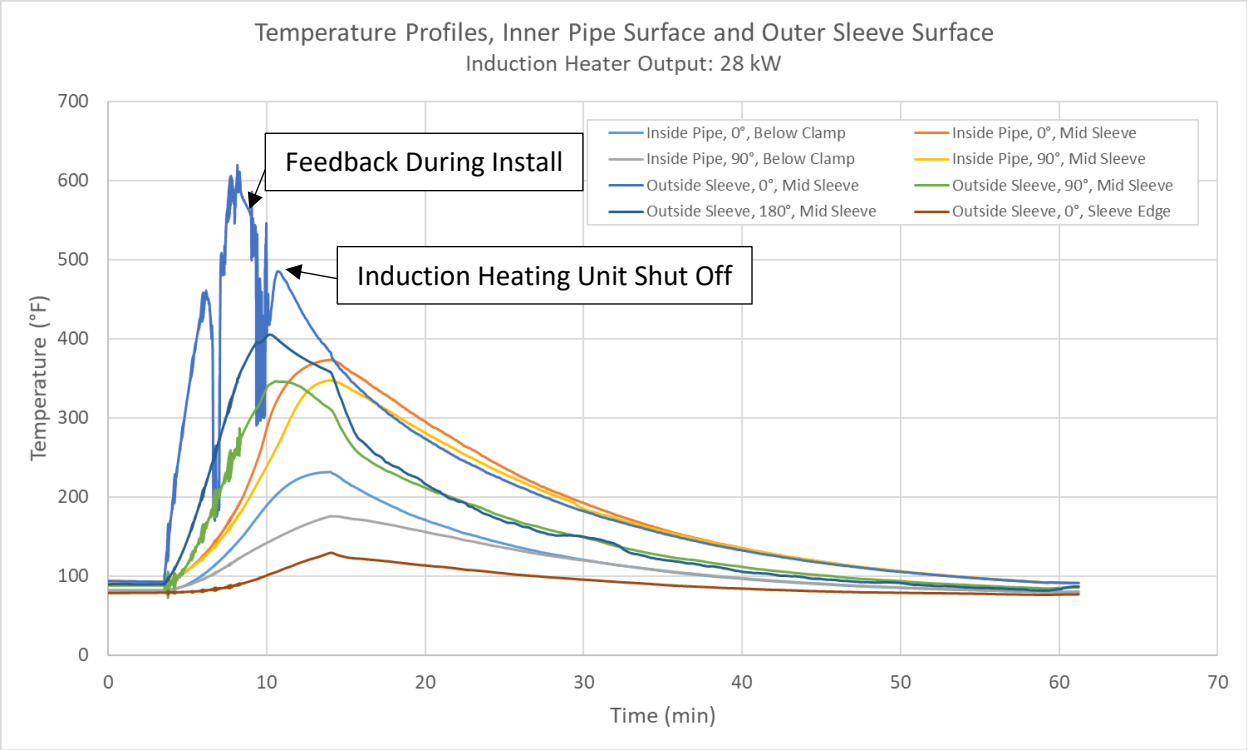


Figure 2-5: Plot of temperature vs time with an induction heater output of 28 kW.

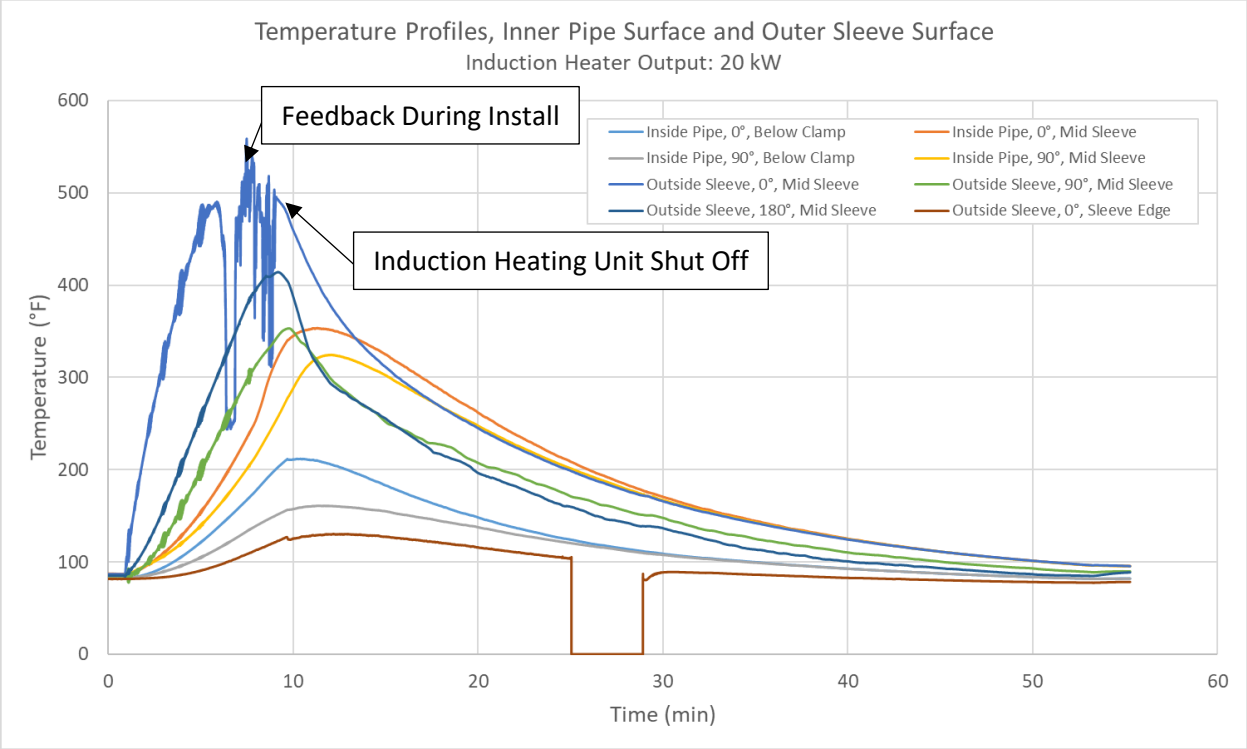


Figure 2-6: Plot of temperature vs time with an induction heater output of 20 kW.

3.0 FULL-SCALE TESTING

A series of full-scale tests were performed to further document the ability of the Compression Sleeve to place the carrier pipe in compression at the maximum operating pressure. The test matrix shown in Table 3-1 was utilized in this study. The following subsections discuss the sample geometry, test plan, test results, and the post-test metallurgical examination of all samples.

Table 3-1: Sample Configuration

Sample #	Notch Depth (%)	Condition
1	50	Ambient Install
2		
3		Flowing Water during Install
4		

3.1 Sample Geometry

Four (4) eight-foot-long full-scale test vessels were fabricated using nominal 12.75-inch OD x 0.188-inch WT, API 5L Grade X52 material manufactured via the high frequency electric resistance welded (HF-ERW) process. One three-inch-long electric discharge machining (EDM) notch was placed at the test vessels mid-length coinciding with the ERW seam weld. The EDM notch was installed to a depth that was approximately 50% of the nominal wall thickness.

3.2 Test Plan

The test plan, described below, includes pre-cycling, installation of the Compression Sleeve, pressure cycling of the repair sample, and burst testing (if sample survives cycling). Each part of the test plan is described below.

Pre-cycling:

1. Install clip gages across the EDM notch to monitor crack growth.

2. Sample installed in ADV Integrity's pressure containment boxes and cycled between 150 psig to 1104 psig (10% – 72% SMYS) until clip gage indicates growth (estimated to be 500 cycles or 0.002-inch displacement.

3. Heat tint notches after growth to indicate EDM notch and pre-crack depth, shown in Figure 3-1.

4. Strain gages were installed on the base pipe per Figure 3-5 to monitor strain and temperature during sleeve installation.



Figure 3-1: Photograph during heat tinting of EDM notch after completing pre-cycling.

Compression Sleeve Install:

Compression sleeves were installed following the Allan Edwards install procedure. A few key steps in this process are listed below:

1. A polymeric hardenable fill material was locally installed around EDM notch to assist with load transfer between the sleeve and pipe, as shown in Figure 3-2.

2. Sleeve was installed and the gap between the two sleeve halves at the weld bevel was measured using a tapered gap gage, shown in Figure 2-1.

3. Induction heater blanket was installed over the sleeve and heater output was set to 35 kW (determined to be most advantageous based on results from the mockup tests), shown in Figure 3-3.

4. Sleeve gap was measured using tapered gap gage upon the induction heater thermocouples reaching 400 °F.

5. Sleeve was welded using E7018 consumables, shown in Figure 3-4.

The strain gages installed at the edge of the compression sleeve were monitored during installation and cooling of the compression sleeve. A triaxial strain gage was installed and centered on top of the sleeve, as shown in Figure 3-5.

Samples 3 and 4 were installed with flowing water through the pipe to simulate flowing product. The water was between 70 and 75 °F and flowed at approximately 5 gallons per minute.



Figure 3-2: Photograph of hardenable fill install at notch location.

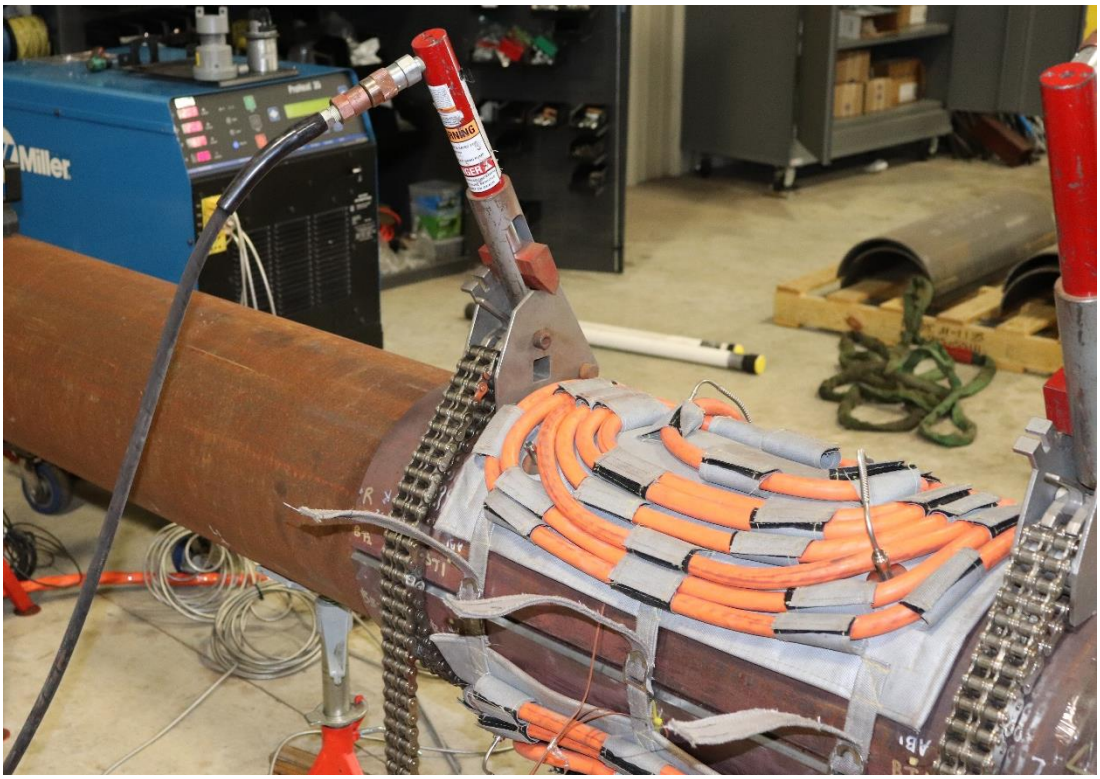


Figure 3-3: Photograph of induction heater set-up.



Figure 3-4: Photograph of long seam welding.

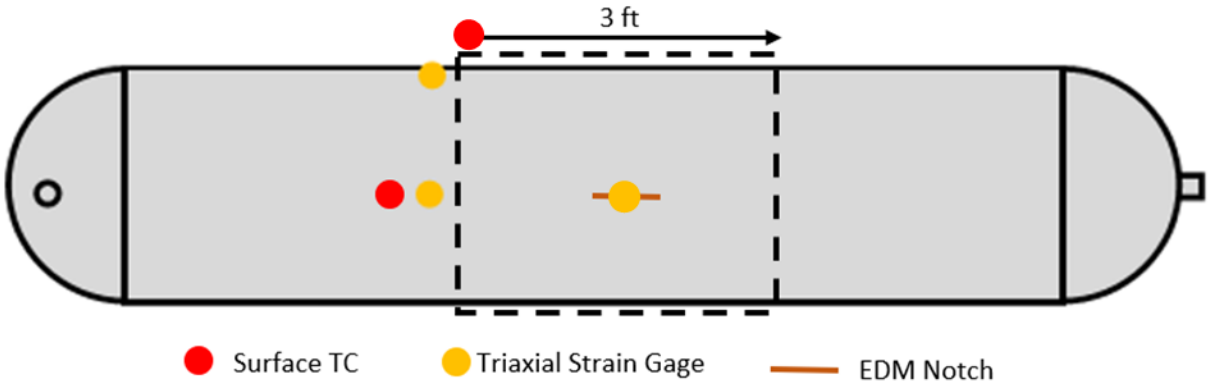


Figure 3-5: Schmatic showing location of strain gages, thermocoupoes, and EDM notch.

Repaired Cycling:

1. Pressure cycle samples to failure or runout of 100,000 cycles.
2. Cycle samples with a pressure range of 150 to 1,104 psi (10 to 72% SMYS).

Burst Test:

1. Perform a burst test if the sample reaches the runout condition of 100,000 cycles.
2. Pressurize sample to failure with 5-minute holds at the following pressures:
    a. 552 psi (36% SMYS)
    b. 1,104 psi (72% SMYS)
    c. 1,533 psi (100% SMYS).

3.3 Test Results

Test samples were instrumented and tested as described in the preceding section. Strain and temperature were monitored during the sleeve install process. Results for all four samples are shown in Figure 3-6 through Figure 3-9, respectively. Several noteworthy items can be interpreted from these plots:

(1) The sleeve temperature experiences an increase during the install as well as during welding. During each welding pass temperatures are generated that are greater than approximately 350 °F. However, the temperature during welding is inconsequential as the potential compression is locked in once the tacks occur (immediately after the temperature increase early in the install).

(2) The samples where water was flowing during the install (Samples 3 and 4) cooled significantly faster than the samples installed in ambient conditions (Samples 1 and 2). This condition is more representative of an install on an active pipeline as the product within the pipe would result in faster cooling.

(3) The strain gage data showed resultant compression once fully cooled; however, the gage experiencing the maximum compressive strain varied from sample to sample. This is likely due to potential ovality in the pipe/sleeve and the interface between the two.

All samples were placed in ADV's pressure containment boxes and cycled to failure or runout of 100,000 cycles. Sample 1 leaked at 8,858 cycles, and Samples 2-4 survived the runout condition. Those samples that survived were burst, with all failures occurring in the base pipe outside the Compression Sleeve at pressures above 100% SMYS, shown in Figure 3-10. A summary of the results is shown in Table 3-2, with an additional unreinforced, 50% EDM notch cycled to failure for comparison.

Table 3-2: Summary of Test Results

Sample #	Number of Cycles	Burst Pressure (psi)	Burst Pressure (% SMYS)
1	8,858	N/A	
2	Runout 100,000 cycles	2,188	142.7
3		2,200	143.5
4		2,195	143.2
Unreinforced[1]	896	N/A	

[1] From ADV PN100068, previous Allan Edwards Compression Sleeve testing

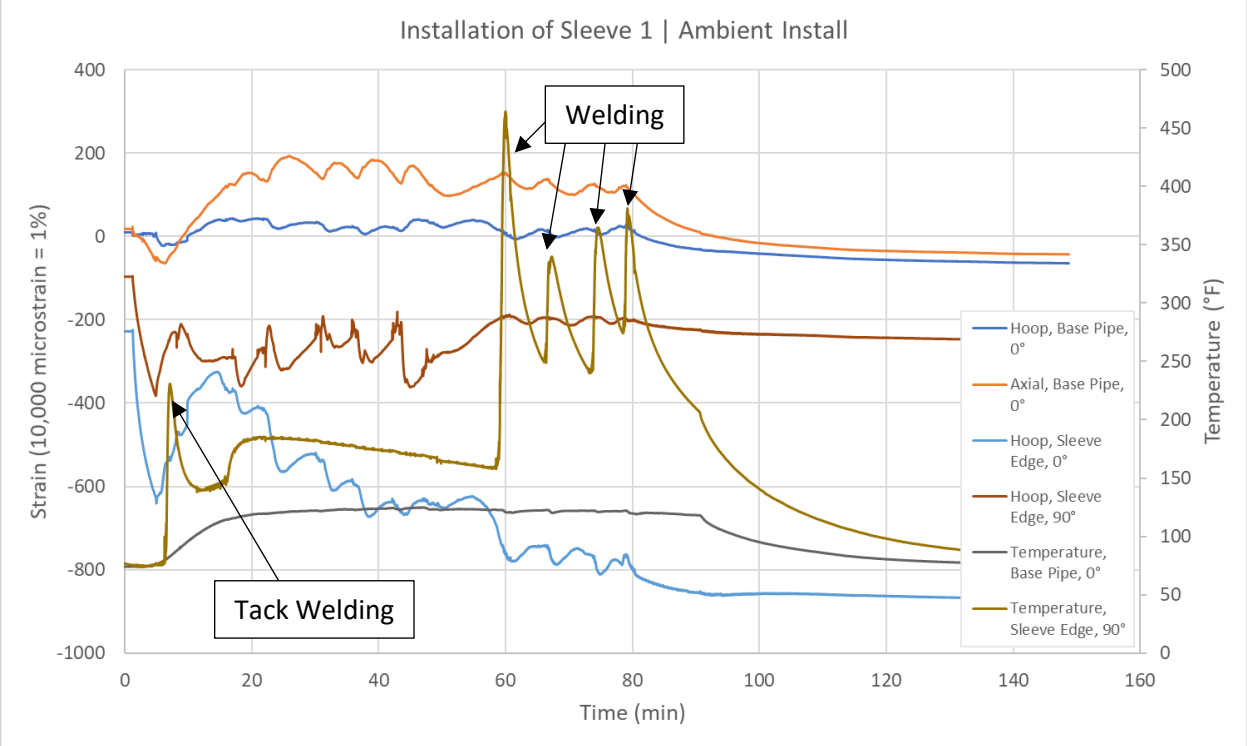


Figure 3-6: Strain and temperature vs time measured during the install of Sleeve 1.

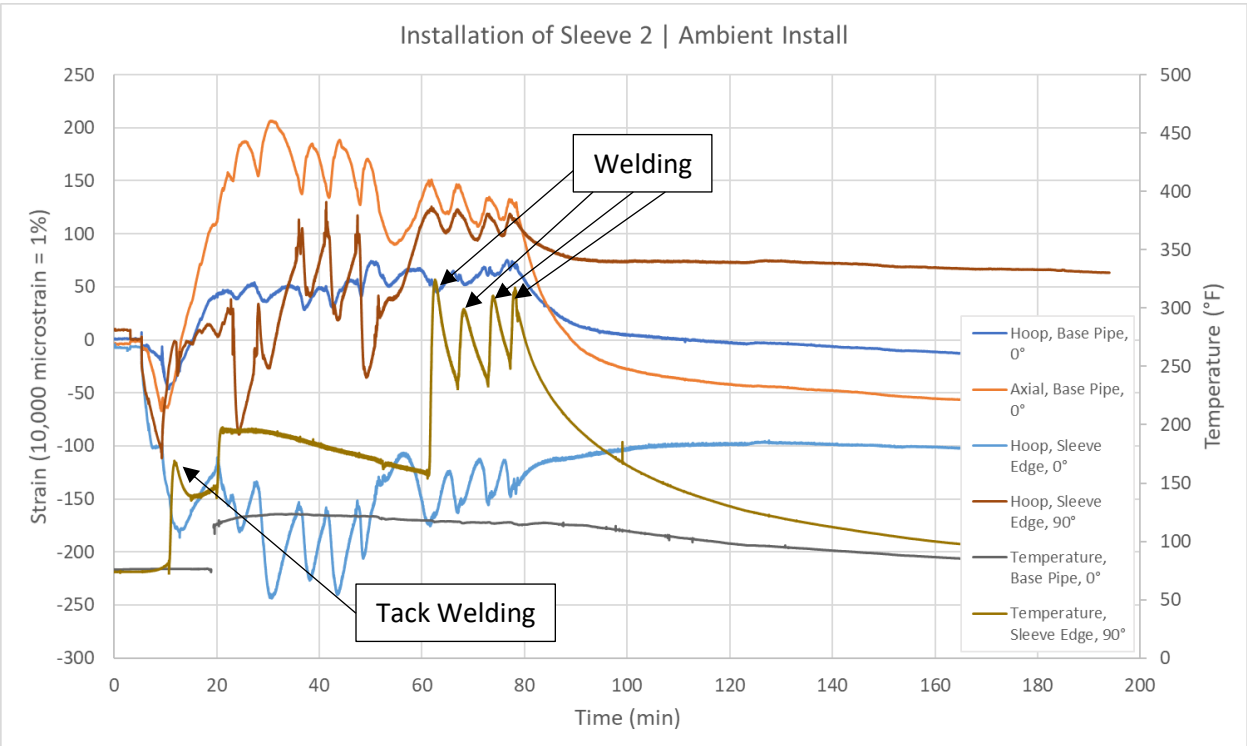


Figure 3-7: Strain and temperature vs time measured during the install of Sleeve 2.

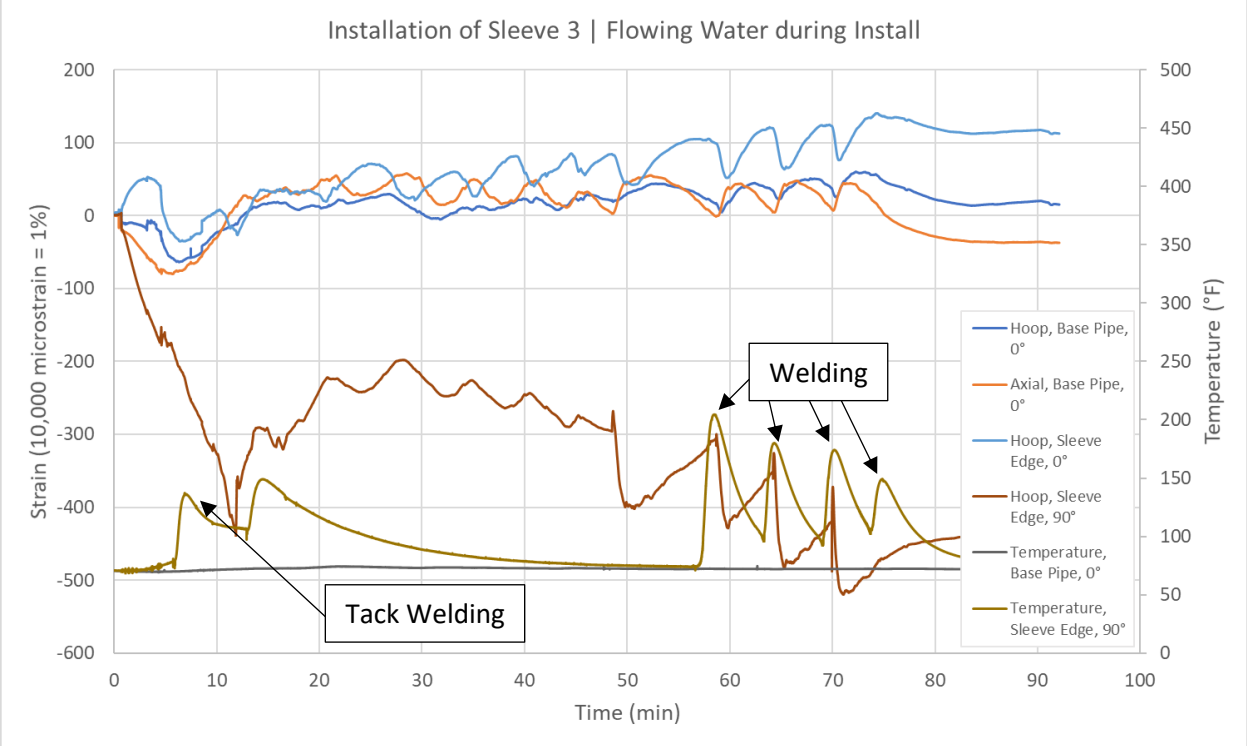


Figure 3-8: Strain and temperature vs time measured during the install of Sleeve 3.

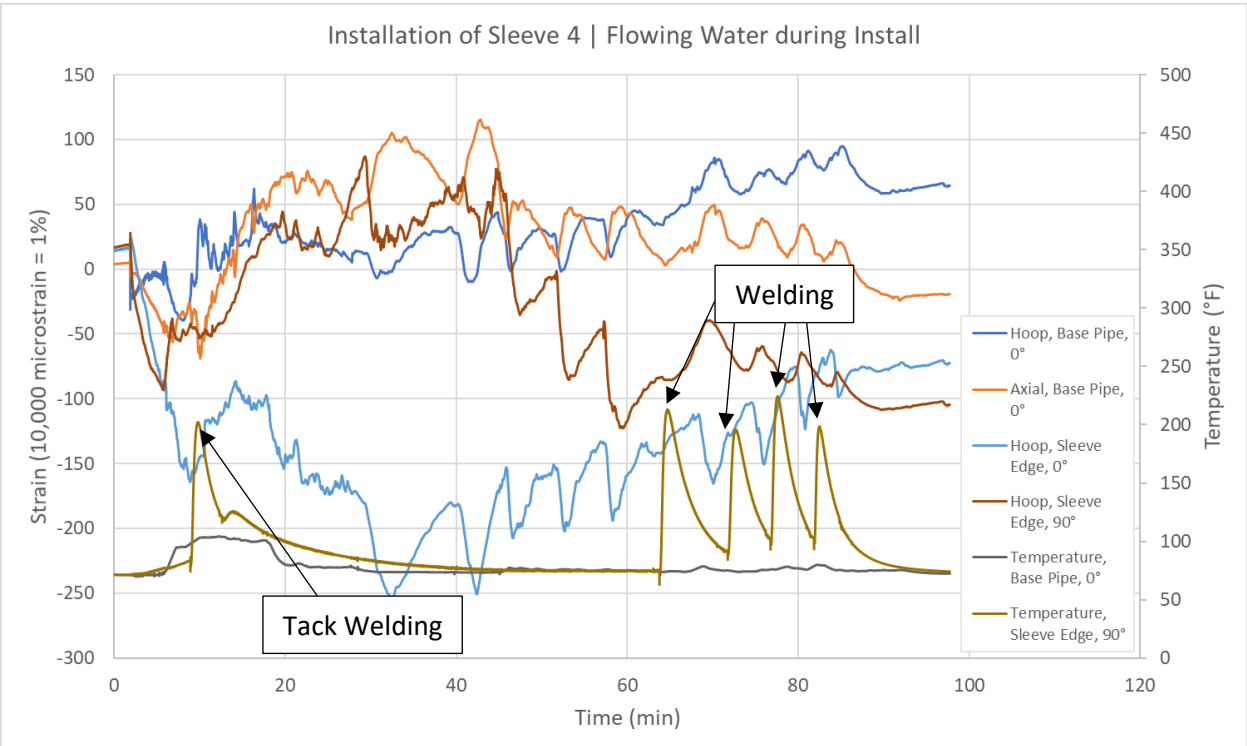


Figure 3-9: Strain and temperature vs time measured during the install of Sleeve 4.

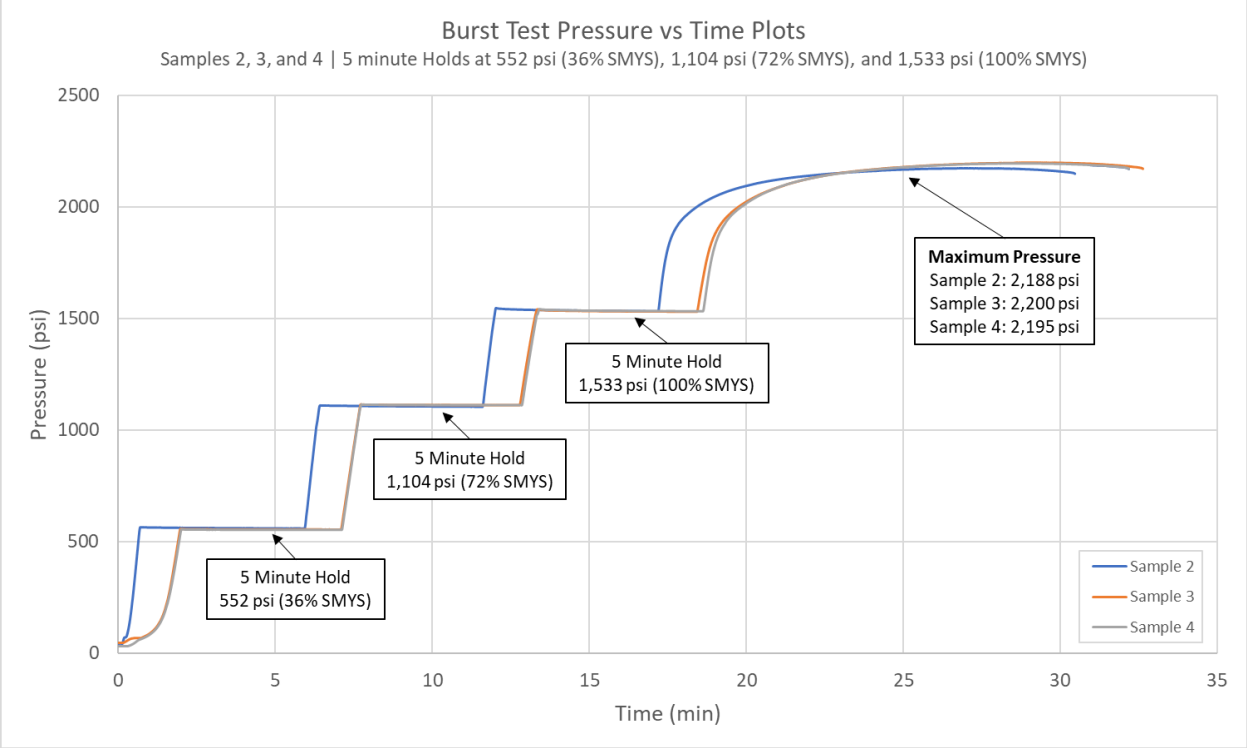


Figure 3-10: Pressure vs time measured during burst testing of surviving samples.

3.4 Metallurgical Examination

After pressure testing ADV removed the EDM notches, further sectioned the pipe via saw cutting, chilled the sample in liquid nitrogen, and broke them open to reveal the fracture surface. The resulting fracture surfaces from all four samples are shown in Figure 3-11 through Figure 3-14, respectively. ADV examined each fracture surface using a stereoscope. The fracture depths listed in Table 3-3 are estimates of the combined EDM "starter" notch and pre-crack depth; however, in some cases the heat tint did not easily distinguish the pre-crack depth.

Sample 1 failed prior to reaching the 100,000 runout condition; however, the pre-crack depth appeared deeper than other fractures when examining the fracture surface. This could indicate an upper limit for crack repair or could indicate differences in fit-up of Sample 1 that resulted in additional growth once repaired.

Table 3-3: Summary of Crack Depths

Sample #	Number of Cycles	EDM Notch Depth (in)	Pre-crack Depth (in)
1	8,858	0.084 (45.0%)	0.050 (26.7%)
2	Runout 100,000 cycles	0.088 (46.8%)	0.027 (14.4%)
3		0.090 (47.9%)	0.026 (13.8%)
4		0.092 (49.2%)	0.016 (8.6%)

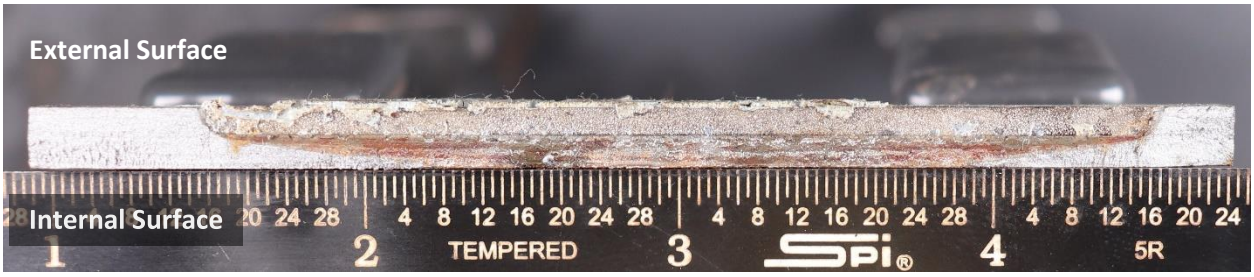


Figure 3-11: Notch from Sample 1. Major numbered scale divisions are inches.

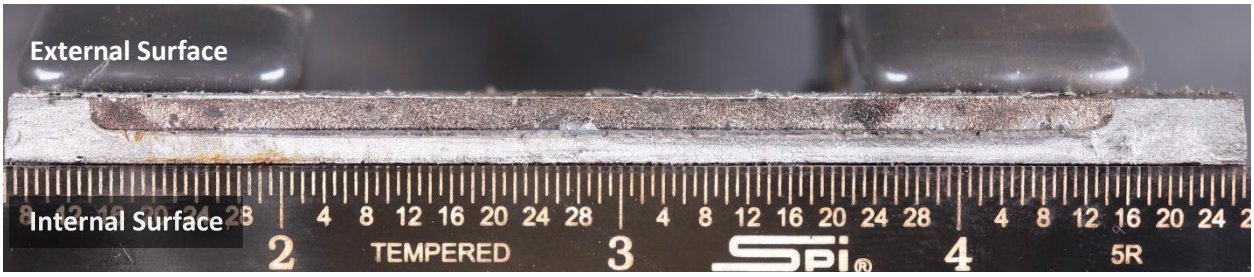


Figure 3-12: Notch from Sample 2. Major numbered scale divisions are inches.

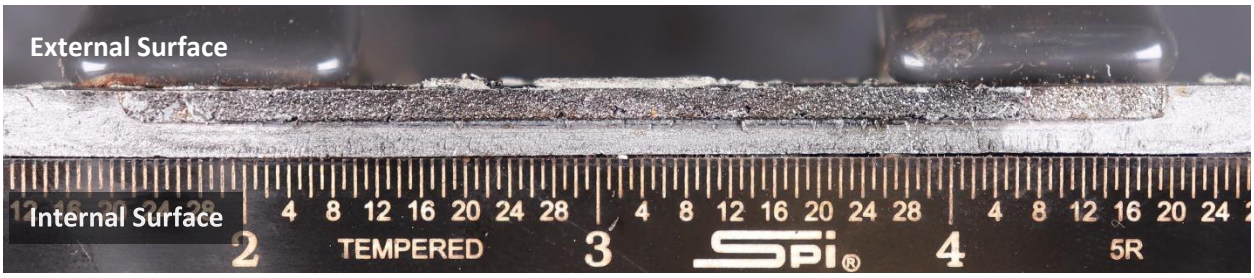


Figure 3-13: Notch from Sample 3. Major numbered scale divisions are inches.

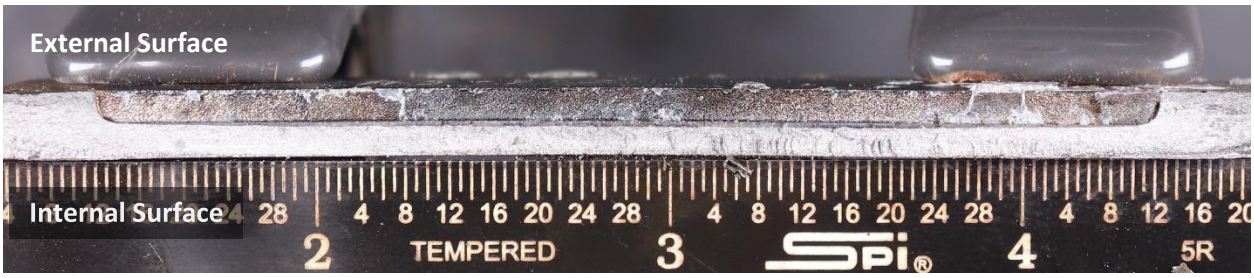


Figure 3-14: Notch from Sample 4. Major numbered scale divisions are inches.

4.0 NUMERICAL MODELING

The numerical modeling efforts manifested in two complementary tasks: 1) theoretical development for the purpose of understanding the primary variables in the mechanics of temperature induced compression (so that finite element analysis is targeted), and 2) finite element analysis (FEA) for detailed interpretation. Both efforts focused on a single combination of the carrier pipe and sleeve.

4.1.1 Pipe and Sleeve Stress Analysis - Concept

There are two key underlying concepts and assumption associated with stress analysis of the compression sleeve system. The first assumption is that the sleeve and carrier pipe remain in perfect contact. The second assumption is that the radial displacement of the pipe is equal to that of the sleeve at the contact interface (i.e., radial displacement compatibility is maintained). In real-world situations both these assumptions may vary due to factors such as pipe ovality, surface roughness, non-uniform temperature distribution etc., but in the present context, these assumptions allow for efficient and reasonable evaluation of the thermal compression concept.

At a fundamental level, the compression sleeve concept relies on the generation of interface pressure between the base/carrier pipe and the sleeve. The higher the interface pressure the higher is the resulting compression on the base pipe. This is shown schematically in Figure 4-1.

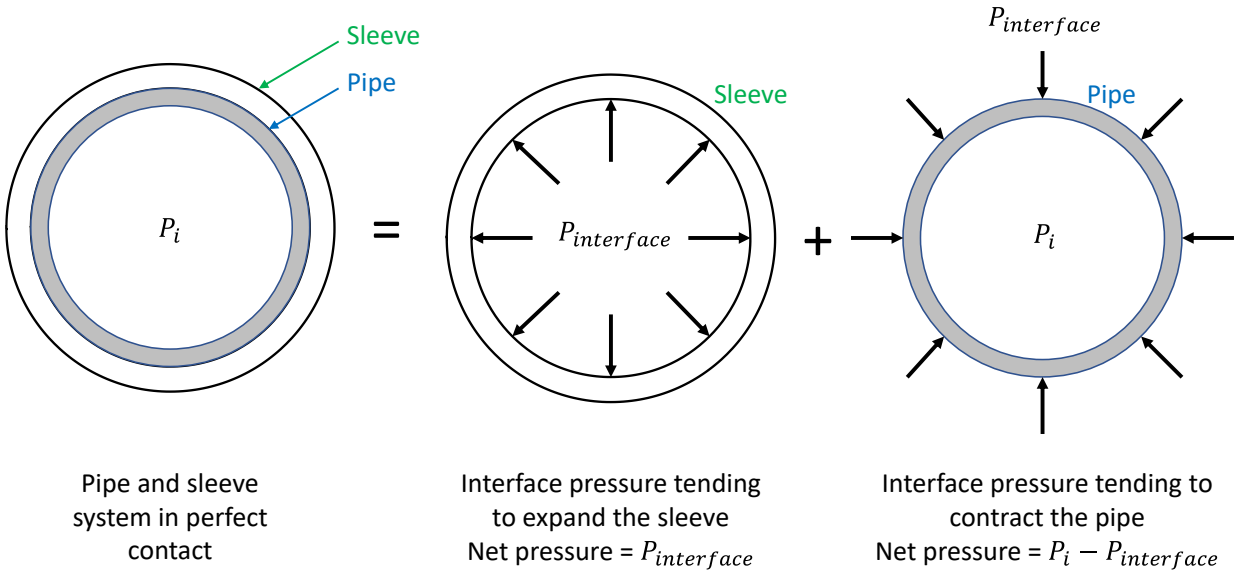


Figure 4-1: Concept of interface pressure between the pipe and the sleeve

For details pertaining to the analytical derivation of the interface pressure and the resulting stresses in the sleeve and the pipe, readers are referred to ADV Report # 100068-RP01-Rev0-113020 (submitted by ADV to Allan Edwards, dated November 30th, 2020) - the equations used in the present work are based on this report.

Three key equations used in the present work are shown below for ease of reference:

$$P_{interface-total} = \frac{\frac{P_i r_{pipe}^2}{t_{pipe} E} + r_{sleeve} \alpha \Delta T_{sleeve}}{\left(\frac{r_{pipe}^2}{t_{pipe} E} + \frac{r_{sleeve}^2}{t_{sleeve} E}\right)} \quad (1)$$

With the total interface pressure known, the hoop stress in the pipe is calculated by:

$$\sigma_{hoop-pipe} = \frac{(P_i - P_{interface-total})\, r_{pipe}}{t_{pipe}} \quad (2)$$

The hoop stress in the sleeve is calculated by:

$$\sigma_{hoop-sleeve} = \frac{P_{interface-total}\, r_{sleeve}}{t_{sleeve}} \quad (3)$$

Where:

P = Internal pressure (psig)
r = Pipe or sleeve radius (inches)
t = Pipe or sleeve thickness (inches)
E = Elastic modulus (psi)
δ = Displacement (inches)
σ = stress; hoop or axial (psi)
ε = strain; hoop or axial

4.2 Finite Element Modeling and Analysis

Two-dimensional (2D), axisymmetric models, finite element (FE) models were created in Abaqus (a general-purpose finite element software program) to simulate geometries of the pipe and sleeve. The pipe dimensions were modeled as 12.75-in OD x 0.188-in wall thickness x 6-ft length and the sleeve dimensions were modeled as 13.5-in OD x 0.375-in wall thickness x 3-ft length. The models (pipe and sleeve) were meshed with a 4-node bilinear axisymmetric quadrilateral element (type CAX4R), which capture the in-plane and out-of-plane behavior. A schematic of the FEA model is shown in Figure 4-2.

The pipe and the sleeve were modeled using linear-elastic material properties with an elastic modulus of 30×10^6 psi, Poisson's ratio of 0.3, and a thermal expansion coefficient of 7.2×10^{-6} 1/˚F. Since the assessment stresses were anticipated to be in the elastic regime, elastic material properties were sufficient to capture the effects of thermal compression and plastic behavior was not defined.

The loading and boundary conditions applied in the FE models simulated a pipe that has end caps and subjected to temperature differentials (based on test data) in addition to internal pressure of 1104 psig (72% SMYS of base pipe).

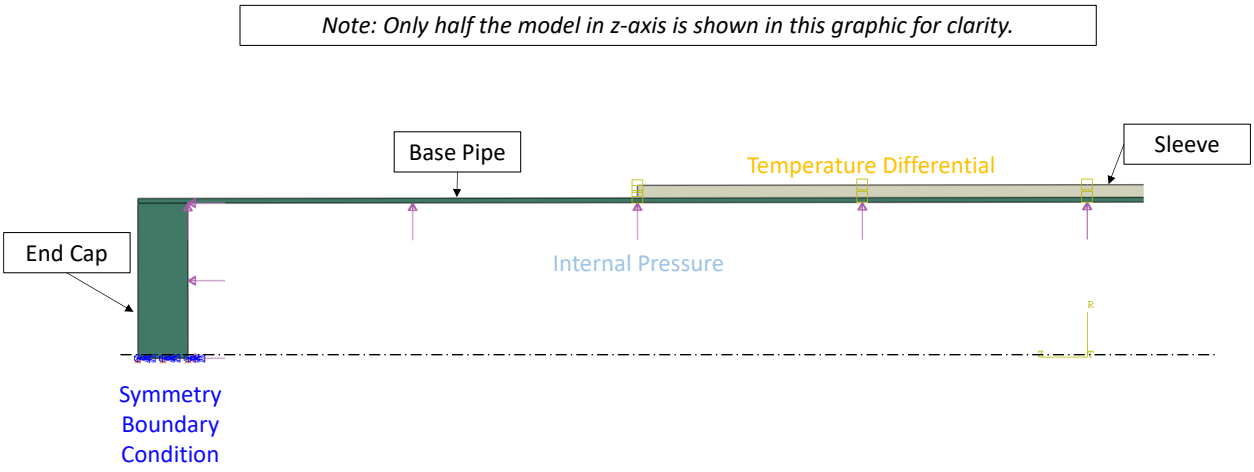


Figure 4-2: Schematic of the FEA model

Two sets of conditions were simulated – one set to represent the conditions for Sample 1 and Sample 2 (sleeve installation at ambient temperature) and the other set to represent conditions for Sample 3 and Sample 4 (sleeve installation with water flowing through base pipe). See Section 3.0 and Table 3-1 for more details on the samples.

For sleeve installation at ambient temperature, a temperature differential of 166 ^{o}F was estimated between the sleeve and the base pipe. Whereas for sleeve installation with water flowing through base pipe, a temperature differential of 316 ^{o}F was estimated between the sleeve and the base pipe. These temperature differential values were based on a combined interpretation of the data collected during the mock-up tests and data collected during the installation of the sleeves on the actual test samples. It should be noted that these temperature differential values represent the average differential over the available data (on account of the fact that the differential varies over the sleeve surface).

4.3 Results and Discussion

As with the analytical formulation, the FEA outcomes can be interpreted in two distinct responses; namely, the thermal response including the heating of the sleeve and subsequent cooling on the base pipe, followed by the mechanical response including the combined response of the system of pipe and sleeve to internal pressure.

With respect to the thermal response, after the heated sleeve cools down, the base pipe under the sleeve is subjected to a compressive stress due to contraction of the compressive sleeve around it. On the other

hand, the sleeve is subjected to a tensile hoop stress as it cools down. These results are shown in Figure 4-3 for a temperature differential of 166 °F (simulating installation conditions for Sample 1 and Sample 2).

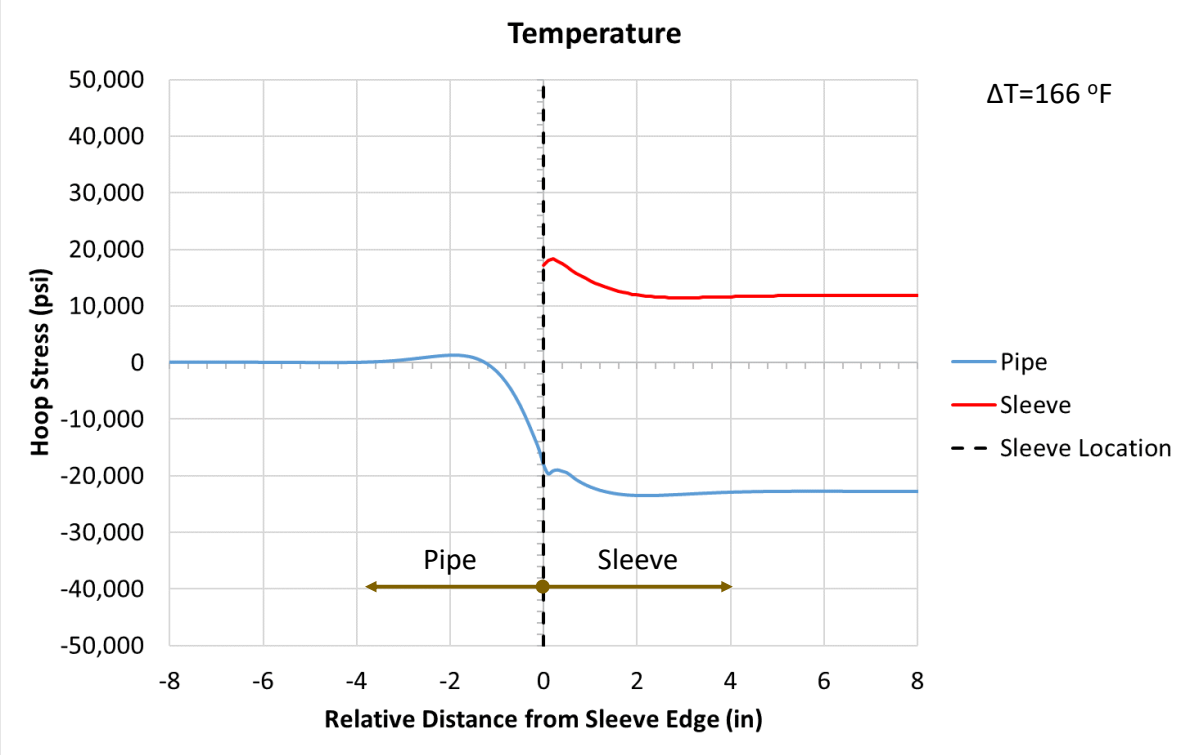


Figure 4-3: Stress profiles due to temperature differentials, ΔT = 166 °F

With respect to the mechanical response due to pressure, the internal pressure in the base pipe results in an increased tensile hoop stress in the base pipe, but at a magnitude lower than the compressive hoop stress induced by the sleeve. For the sleeve, the internal pressure further increases the tensile hoop stress over that introduced by the thermal response. The result is that the net state of hoop stress in the base pipe is compressive, whereas that in the sleeve is tensile. This is illustrated in Figure 4-4 for an internal pressure of 1104 psig (this pressure corresponds to 72% SMYS of the base pipe and was the target high pressure during cyclic full-scale testing of all 4 samples). With respect to Figure 4-4, results showed that the net compressive hoop stress in the base pipe is calculated to be approximately -7.0 ksi (negative sign indicates compression), and the net tensile hoop stress in the sleeve is calculated to be approximately 22.2 ksi.

Figure 4-5 shows a comparison between the thermal response and the total response (thermal + pressure) to facilitate a comparison between the relative magnitudes of the stresses due to each type of response.

The analysis was repeated with a temperature differential of 316 °F (simulating installation conditions for Sample 3 and Sample 4) with 1104 psig internal pressure. The results are shown in Figure 4-6 through Figure 4-8. For 316 °F differential, the net compressive hoop stress in the base pipe is calculated to be

approximately -27.8 ksi, and the net tensile hoop stress in the sleeve is calculated to be approximately 32.9 ksi.

The results for the two temperature differentials are compiled together and presented in Figure 4-9 along with linear extrapolation and interpolation for other temperature differentials. The graphical form of the solution illustrated in Figure 4-9 can be used for other temperature differentials (based on actual installation measurements) to predict the net state of stress in the sleeve and the pipe after installation and pressurization.

To ensure/check that the FEA outcomes are reasonable, the results were compared against spreadsheet-based analytical solutions based on Equations 1, 2, and 3 presented previously. A summary of the comparison is shown in Figure 4-10. The results showed very good correlation between the two approaches. The small differences in the net stresses between the spreadsheet-based calculations and FEA were attributed to the pressure end load effects that were correctly accounted for in the FEA but ignored for the spreadsheet-based calculations.

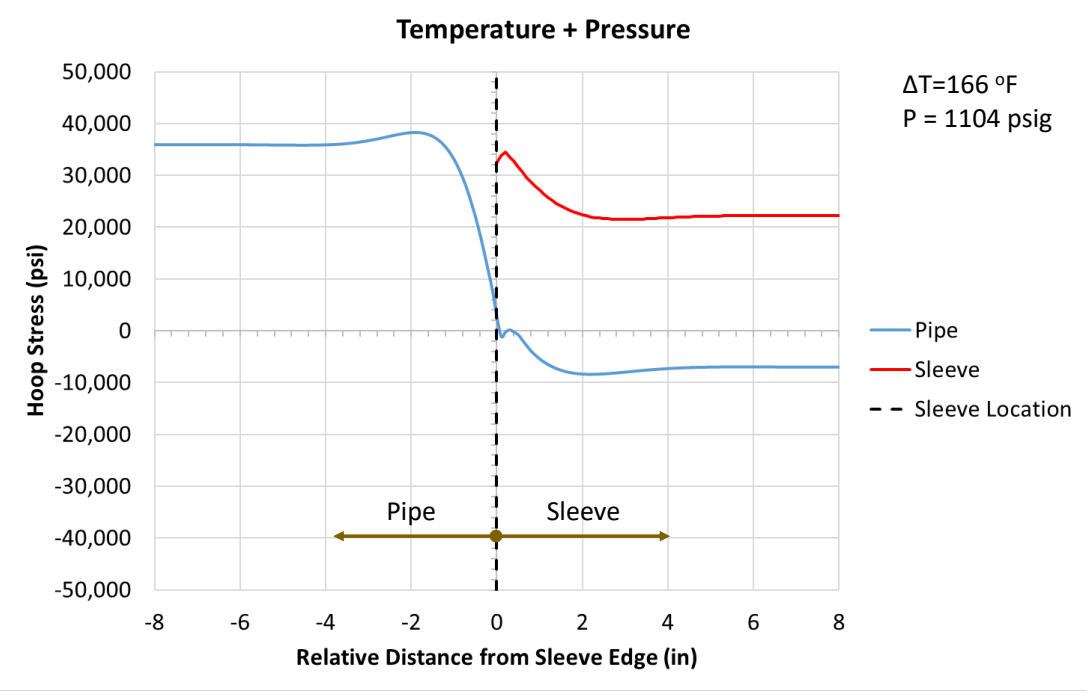


Figure 4-4: Stress profiles due to temperature differentials + pressure, ΔT = 166 °F, P = 1104 psig

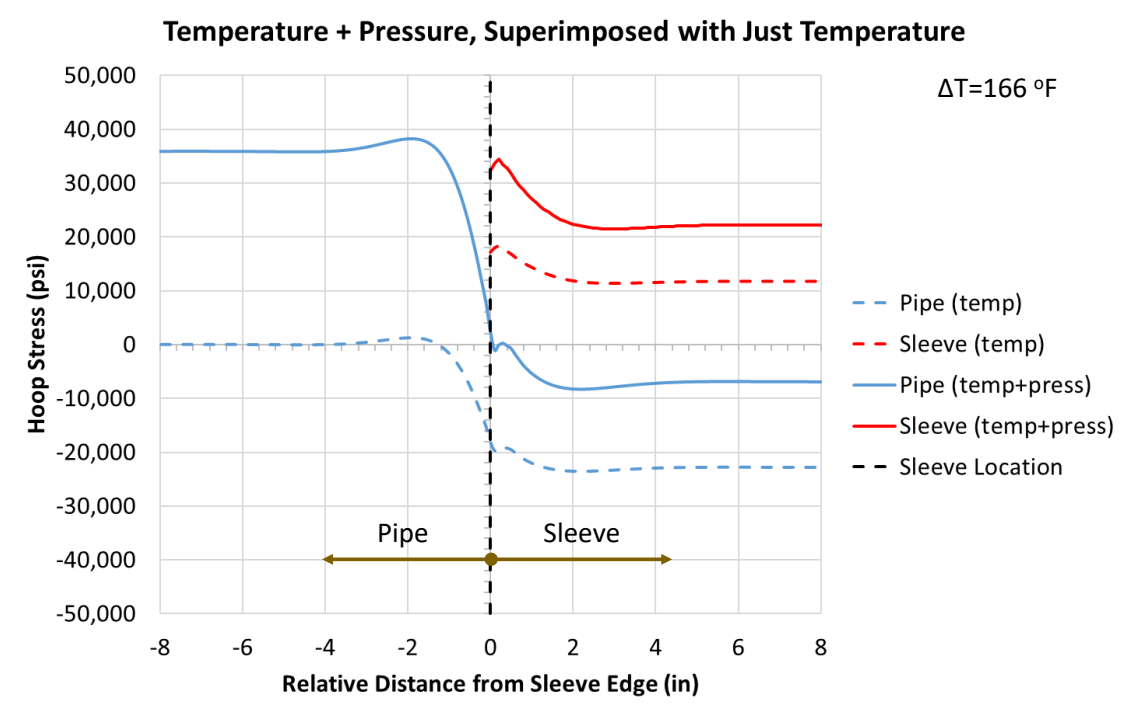


Figure 4-5: Comparison of stress profiles – temperature + pressure vs only temperature, ΔT = 166 °F

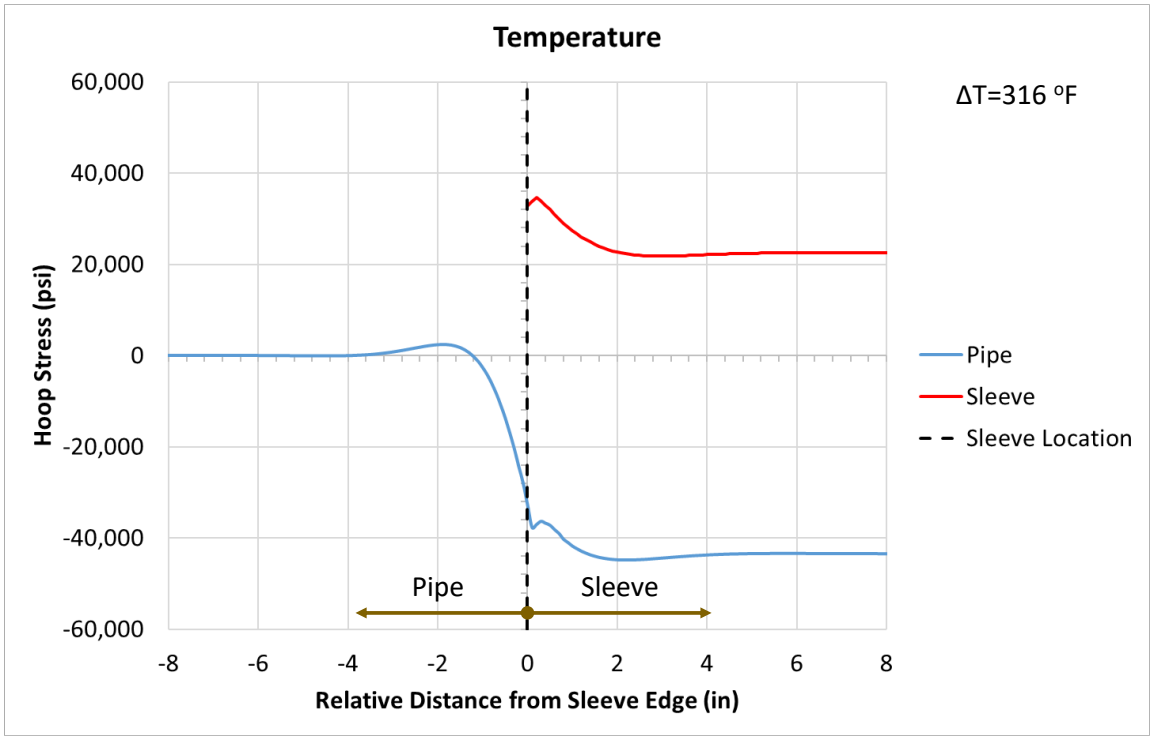


Figure 4-6: Stress profiles due to temperature differentials, ΔT = 316 °F

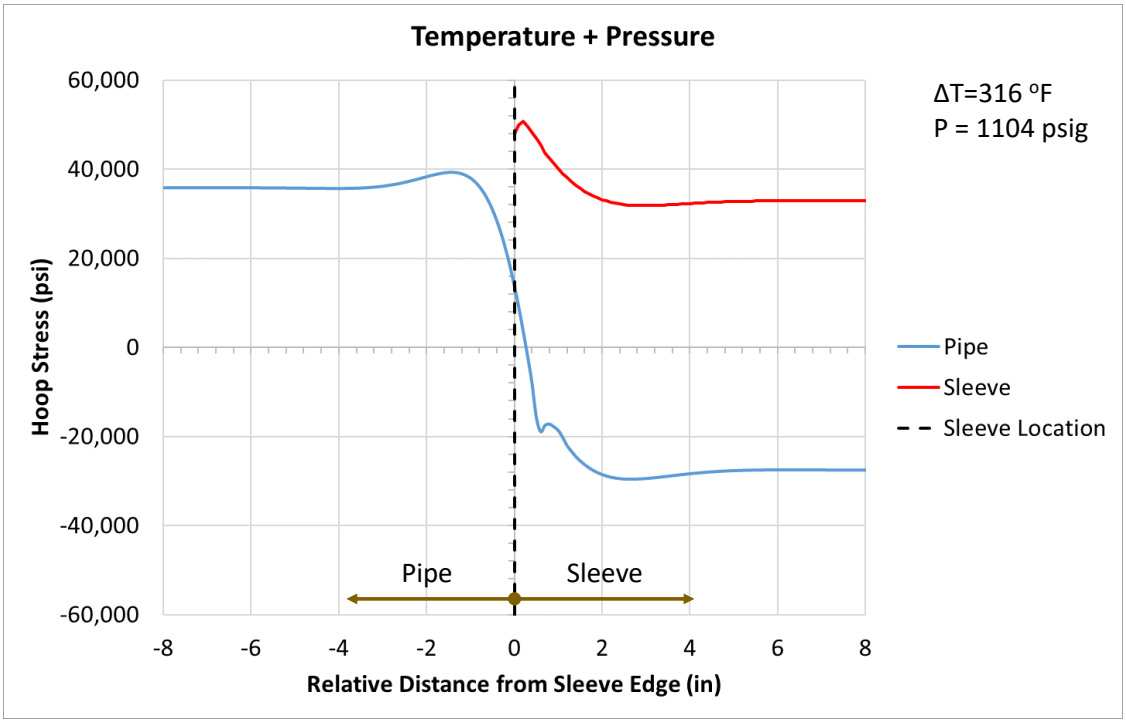


Figure 4-7: Stress profiles due to temperature differentials + pressure, ΔT = 316 °F, P = 1104 psig

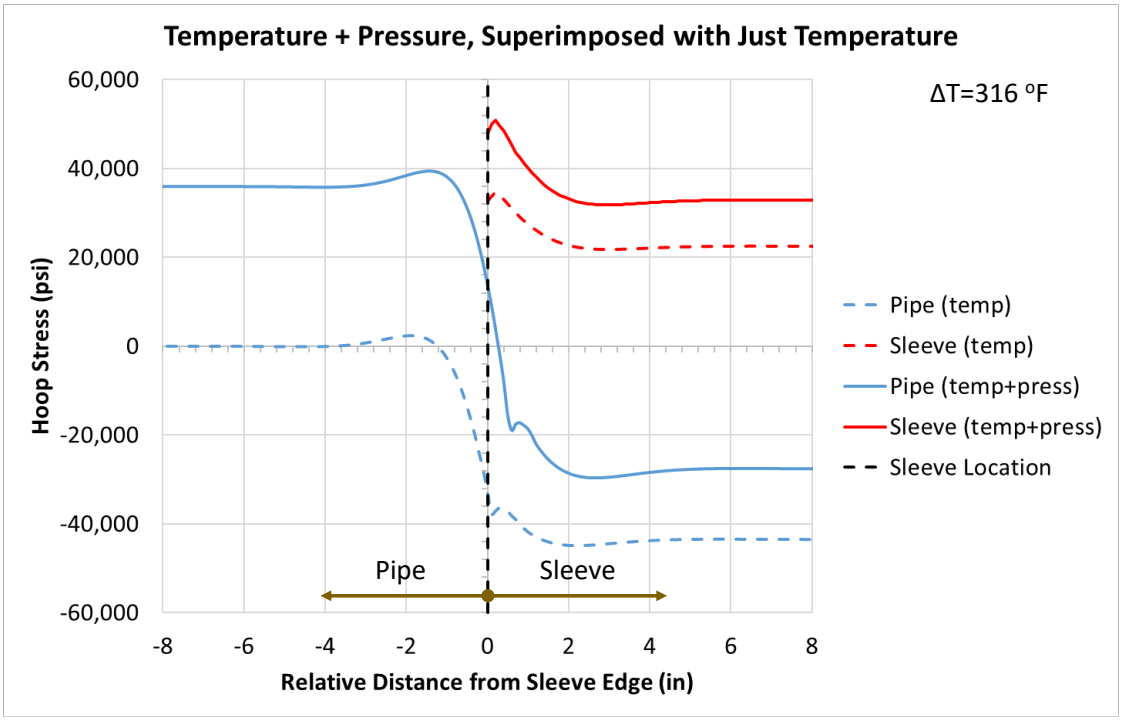


Figure 4-8: Comparison of stress profiles – temperature + pressure vs only temperature, ΔT = 316 °F

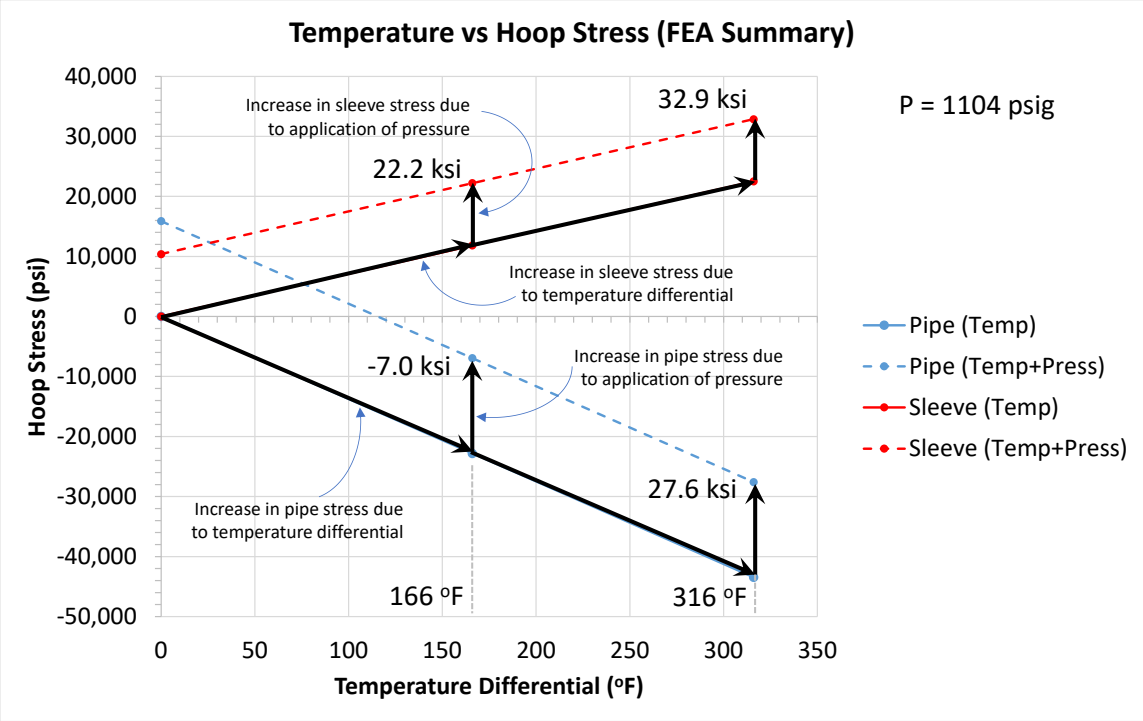


Figure 4-9: Summary of FEA results for pipe and sleeve stresses at various temperature differentials

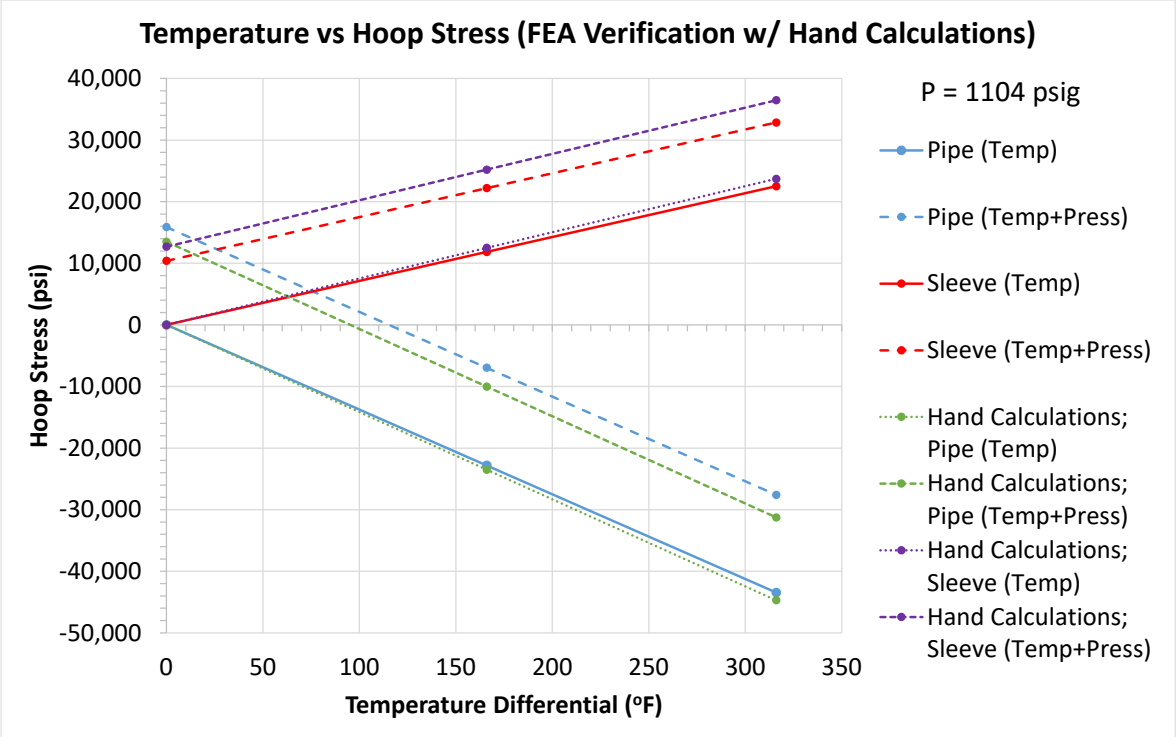


Figure 4-10: Summary of FEA results for pipe and sleeve stresses – verification

4.4 Interpretation of Measured Gap Data for Estimating Sleeve Performance

As discussed in Section 2.0, sleeve gaps were measured using a tapered gap gage during the second set of mock-ups and the results reported in Table 2-2. In cases where strain measurement is difficult or impractical, or inconclusive (as in the present case), the measured gap data can serve as a reasonable proxy for the estimated compressive effect of the sleeves.

This is based on the fundamental understanding that the gaps between the sleeves will close (measured gap will be smaller) as the sleeve heats up relative to the pipe. Conceptually, for a thermal compressive sleeve to work, the basic premise is that the sleeve should be hotter than the pipe – the observation of sleeve gap closure data during installation confirms this premise and serves as an assurance the sleeve is working as intended.

When processed with thermal expansion coefficients, the measured gap closure can be interpreted as an increase in length of the sleeve due to an "apparent" sleeve temperature increase. This apparent sleeve temperature can then be used in Equation (1) for estimating the net compressive effect on the pipe. This interpretation of temperature is termed "apparent" because instead of representing the actual temperature, it collectively represents the net effect of various physical responses due to temperature such as sleeve and pipe temperatures, their relative expansions, clamping pressures, etc. Using the gap information provided in Table 2-2, and interpreting apparent temperatures for the respective gap data, the stresses in the pipe and sleeve were calculated; the results are shown in Table 4-4. The table also shows the net development of stresses in the sleeve and the pipe if the pipes were to be pressurized to their respective 72% SMYS pressures after the sleeve installation (the three right-most columns in the table).

Table 4-4: Summary of Calculated Stresses in the Pipe and the Sleeve Using Measured Gap Data

Sample		Total Average Gap Δ (in)	Apparent Sleeve Temp (°F)	Hoop Stresses After Cooldown, No Pressure (ksi)		Internal Pressure (psig)	Net Hoop Stresses After Pressure Application (ksi)	
OD	#			Sleeve	Pipe		Sleeve	Pipe
24 inch	1	0.050	93.0	9.1	-10.6	973	26.2	6.9
	2	0.049	91.2	8.9	-10.4	973	26.0	7.2
12 inch	1	0.063	217.9	16.4	-30.8	1104	29.1	-17.4
	2	0.048	164.7	12.4	-23.3	1104	25.1	-9.8
	3	0.084	291.3	21.9	-41.2	1104	34.6	-27.8
	4	0.066	228.9	17.2	-32.4	1104	29.9	-18.9

5.0 DISCUSSION AND SUMMARY

Three of the four installed Compression Sleeves resulted in sufficient reinforcement to prevent crack growth. Relating 100,000 pressure cycles at the tested range (10 to 72% SMYS) results in an equivalent 57,764 cycles with a ΔP of 72% SMYS. For some time, the pipeline industry has employed the data compiled by John Kiefner where he classified pressure cycling in four categories based on industry surveys: *Very Aggressive*, *Aggressive*, *Moderate*, and *Light* (refer to data presented in Table 5-1). As noted, a *Very Aggressive* condition will result in 276 cycles per year and a *Light* condition will result in 10 cycles per year assuming a pressure range of 72% SMYS. Gas transmission pipelines typically experience minimal cycling, so a *Light* pressure cycle condition is appropriate. Accounting for a safety factor of 5, results in an approximate cyclic life tested of 42 years in a Very Aggressive pressure cycling regime and 1,155 years in a Light pressure cycling regime – both significantly long periods when examining the 100,000 cycles each sleeve survived in this study. It should be noted that Samples 2 through 4 did not fail; therefore, the fatigue life would be significantly longer than the life mentioned above (achieving more than 100,000 pressure cycles).

Table 5-1: Annual Cyclic Pressure Conditions Based on Kiefner Study Industry Survey[1]

(Estimated number of annual cycles as a function of cyclic pressure condition)

Percent SMYS	Very Aggressive	Aggressive	Moderate	Light
72	20	4	1	0
65	40	8	2	0
55	100	25	10	0
45	500	125	50	25
35	1000	250	100	50
25	2000	500	200	100
Total	3660	912	363	175
Single equivalent number of annual cycles with ΔP as noted				
72%	276	67	25	10
61%	512	124	47	18
36%	3,683	889	337	128

The crack-like feature in one sample (Sample 1) was considerably deeper than the other three and therefore could set a limit for the repairable depth with this system. This sample experienced an approximately 10x fatigue life extension when compared to the unreinforced sample from the previous testing scope. Accounting for a safety factor of 5, the 8,858 cycles results in an approximate cyclic life tested of 6.5 years considering a Very Aggressive pressure cycling regime and 177 years with a Light pressure cycling regime.

[1] Kiefner, J.F. et al., Estimating Fatigue Life for Pipeline Integrity Management, Paper No. IPC04-0167, Presented at the International Pipeline Conference, Calgary, Canada, October 4–8, 2008.

Based on the data collected during mock-up tests, sleeve installation process on full-scale test samples, and subsequent cyclic tests, it can be inferred that the installed sleeves performed as expected. The relatively early failure of Sample 1 is likely an outlier due to an assignable cause (such as deeper initial notch compared to notches in the other samples or non-uniform material properties in the vicinity of the notch); additional data and/or detailed interpretation of the existing data may be required to narrow down on the possible causes for the early failure associated with this sample. Other observations and inferences are listed below:

(1) Data from the mock-up tests are indicative of the fact that the clamping pressure may not be a consistent and significant driver in the overall compression sleeve system performance. Based on the strain data shown in Figure 2-3, the strains in the pipe under the sleeve were not consistently compressive in nature upon the application of clamp pressure. In addition to inherent imperfections in the pipe ovality, it is also likely that the initial contact between the base pipe and the sleeve is imperfect where the sleeve only contacts the pipe at the top and the bottom regions (see Figure 5-1). In this scenario, application of clamp pressure on the sleeve will ovalize the pipe leading to tensile strains at 90° locations (contrary to the expectation of uniform compressive strains in the base pipe). Upon releasing the clamp pressure (even after the sleeve halves are tacked), the system will redistribute the strains along the base pipe circumference as long as the deformations are in the elastic regime. Rigorous test data to conclusively establish this phenomenon are not available but based on the relatively small change in strains observed in Figure 2-3 (especially for repeat loadings), it can be hypothesized the redistributed strains after the removal of clamping pressure is unlikely to be significant.

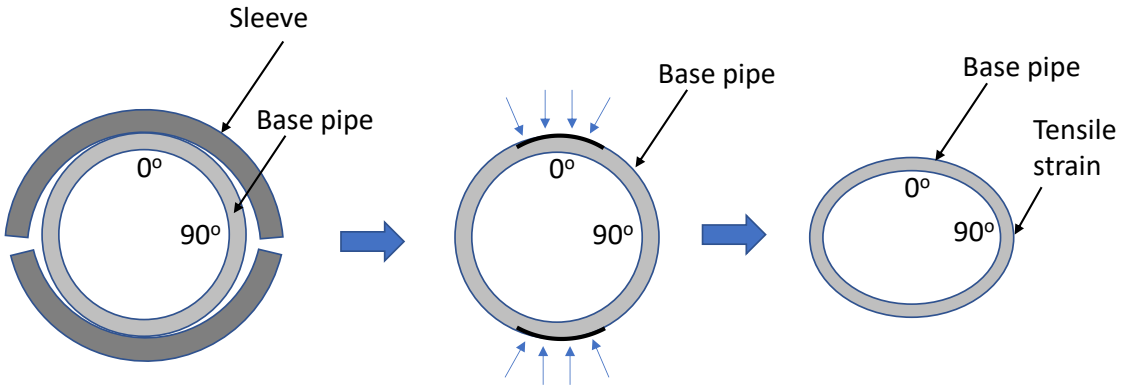


Figure 5-1: Possibility of base pipe ovalization during clamping of the sleeve on the base pipe

(2) It can be observed from the stress profiles shown in Figure 4-3 through Figure 4-8 that at stresses in the base pipe and the sleeve show a nonlinear response near the edge of the sleeve (due to edge effects). This region of nonlinear stress distribution extends approximately 4 to 5 inches from the edge of the sleeve in either direction. In real-world applications, it is likely that the temperature differential at the edge of the sleeve is lower than that in the rest of the sleeve resulting in a slightly subdued nonlinear response; however, from a design perspective, it is recommended that sleeve lengths be designed to account for at least 6 inches of nonlinear stress

response on either side of the edge. i.e., the edge of the sleeve should be at least 6 inches away from any potential stress rise in the pipe (for example, a girth weld).

(3) During the sleeve installation process, installers measured the gap between the sleeve halves using tapered gap gages. Although this measurement provides a qualitative (and relative) measure of gap closure, in light of Figure 5-1, part of the gap closure may be likely due to partial ovalization of the base pipe in addition to the "squeezing" of the free longitudinal edges of the sleeve halves. To allow the gap measurements to be more useful in the field (as a measure of the amount of target compression), it is recommended that the gap measurements be performed before and after heating the sleeves *at the same clamping pressure* – this will ensure that the thermal effect is isolated from the clamping pressure effect and can be correlated to the effective thermal gradient between the sleeve and the base pipe. With this approach, guidance can be provided that correlates the measured gap to the expected compression in the base pipe, performed via the installation calculator. This is demonstrated in the discussion and results provided in Section 4.4.

    a. Additional statistical characteristics can be generated for gap data that can be used for statistical control of the installation process (serving as a quality assurance measure in the field). For example, installations with gap closures that fall above a certain threshold based on the desired confidence levels can be deemed as "PASS".

Other operational considerations regarding a Type A Compression Sleeve are as follows:

(1) The installers should consider the effects of seam welds with raised caps (e.g., DSAW, EFW, etc.) or girth welds in the event the Compression Sleeve has to be installed over such features. There are two approaches to this repair attempt: (1) grind raised profiles on the carrier pipe, which is outside the scope of this project and should follow an operator's standard procedures or (2) grind (or manufacturer) relief grooves into the internal surface of the sleeve. This can be accomplished by using a soap stone to mark the location of the raised caps, fit-up the sleeve, remove the sleeve then grind a relief prior to re-installation. Once completed, the remaining wall thickness along the relief groove should be determined for input into repair calculator.

(2) The ability of a Compression Sleeve to properly function is dependent on the carrier pipe under the sleeve to maintain a relatively straight profile and minimize ovality. The API 5L limits for out of straightness and ovality seems appropriate to apply here. API 5L limits out of straightness to 0.2% of the measured length (so for a three-foot sleeve, the max out of straightness would be 36 inches x 0.002 = 0.072 inch). API 5L limits of ovality is specified as 2%.

(3) Three general approaches seem reasonable in the event an unsuitable result is determined though the repair calculator: (1) revalidate the inputs into the calculator including the level of stress that's required at the maximum operating pressure of the pipeline, (2) convert the sleeve to a Type B sleeve by completing the circumferential end welds, or (3) remove the sleeve by

grinding and attempt a new repair. The most appropriate path forward should be determined by the operator and follow the operator's standard procedures.